nature portfolio

https://doi.org/10.1038/s41586-023-05845-8

Supplementary information

Depolymerization of plastics by means of electrified spatiotemporal heating

In the format provided by the authors and unedited

Supplementary Information for

Depolymerization of plastics by means of electrified spatiotemporal heating

Qi Dong[1†], Aditya Dilip Lele[2†], Xinpeng Zhao[1†], Shuke Li[1†], Sichao Cheng[3], Yueqing Wang[4], Mingjin Cui[1], Miao Guo[1], Alexandra H. Brozena[1], Ying Lin[2], Tangyuan Li[1], Lin Xu[1], Aileen Qi[1], Ioannis G. Kevrekidis[5], Jianguo Mei[6], Xuejun Pan[4], Dongxia Liu[3], Yiguang Ju[2*], Liangbing Hu[1,7*]

[1]Department of Materials Science and Engineering, University of Maryland, College Park, Maryland 20742, United States

[2]Department of Mechanical and Aerospace Engineering, Princeton University, Princeton, New Jersey 08544, United States

[3]Department of Chemical and Biomolecular Engineering, University of Maryland, College Park, Maryland 20742, United States

[4]Department of Biological Systems Engineering, University of Wisconsin-Madison, Madison, Wisconsin 53706, United States

[5]Department of Chemical and Biomolecular Engineering, Department of Applied Mathematics and Statistics, Johns Hopkins University, Baltimore, Maryland 21218, United States

[6]Department of Chemistry, Purdue University, West Lafayette, Indiana 47907, United States

[7]Center for Materials Innovation, University of Maryland, College Park, Maryland 20742, United States

[†]These authors contributed equally to this work.

[*]binghu@umd.edu; yju@princeton.edu

Table of Contents

Supplementary Table 1

The yield (or selectivity) of PP depolymerization in our work (using the electrified STH approach under far-from-equilibrium conditions) compared to literature reports.

Reaction Conditions or Catalyst	Yield or Selectivity (%)	Refs.
HZSM-5	20.1	16
HZSM-5	22	16
HZSM-5	18.6	16
HZSM-5	16.8	16
HZSM-5	23.5	15
HUSY	8.1	15
HMOR	15.6	15
SAHA	3.8	15
MCM-41{Al}	7.3	15
Zeolite Y with gas oil	9.5	17
Zeolite Y with gas oil	8.7	17
Zeolite Y with gas oil	8.4	17
Zeolite Y with gas oil	4.3	17
Zeolite Y with hydrotreated vacuum gas oil + gas oil	9.1	17
Zeolite Y with hydrotreated vacuum gas oil + gas oil	7	17
Zeolite Y with hydrotreated vacuum gas oil + gas oil	7	17
Zeolite Y with hydrotreated vacuum gas oil + gas oil	5.4	17
Silica with light cycle oil	7.5	19
Non-catalytic	10.4	18
Electrified STH	35.5	This work

Supplementary Table 2

The yield of PP depolymerization under various reaction conditions reported in this work. The uncertainty values of the monomer yield denote standard deviation for $n \geq 3$. See Methods for detailed calculations about the uncertainty value of the peak temperature.

Reaction Conditions	Monomer Yield (%)	Figure
STH, 0.11 s on, 0.99 s off, T_{peak} = 600 ± 9 °C, PP beads, 0.1 g	35.5 ± 6.2	3a, b, d, e
Continuous heating, single heater layer placed underneath the reactant reservoir, T = 600 ± 9 °C, PP beads, 0.1 g	16.7 ± 6.0	Control Experiment
STH, 0.11 s on, 0.99 s off, T_{peak} = 600 ± 9 °C, PP beads, operation #1, 0.1 g	35.0	3c
STH, 0.11 s on, 0.99 s off, T_{peak} = 600 ± 9 °C, PP beads, operation #2, 0.1 g	32.5	3c
STH, 0.11 s on, 0.99 s off, T_{peak} = 600 ± 9 °C, PP beads, operation #3, 0.1 g	38.8	3c
STH, 0.11 s on, 0.99 s off, T_{peak} = 600 ± 9 °C, PP beads, operation #4, 0.1 g	35.4	3c
STH, 0.11 s on, 0.99 s off, T_{peak} = 600 ± 9 °C, PP beads, 0.2 g	34.2	3d
STH, 0.11 s on, 0.99 s off, T_{peak} = 600 ± 9 °C, PP beads, 1.0 g	33.8	3d
STH, 0.11 s on, 0.99 s off, T_{peak} = 600 ± 9 °C, commercial PP bag, 0.03 g	34.3 ± 7.5	3e

Supplementary Table 3

Parameters used for the STH operation for different scales of the reaction system and masses of the PP reactant. The scaling factor is based on the PP mass feed, with the initial scale of 0.1 g defined as 1.

Scaling Factor	Carbon Felt Heater Layer			Carbon Felt Reactor Layer			Average Voltage/V	Flow Rate/sccm
	L/mm	W/mm	H/mm	L/mm	W/mm	H/mm		
1 (0.1 g)	25	9	2.3±0.1	13	6	4.7	22	100
2 (0.2 g)	50	9	2.3±0.1	26	6	4.7	32	100
10 (1.0 g)	100	18	2.3±0.1	35	12	4.7	40	1400*

*The flow rate was scaled based on the estimated increase of the system's effective cross-sectional area (i.e., the cross-sectional area of the quartz tube minus the area occupied by the reaction unit, including the carbon felt bilayer structure, the reservoir, and the electrical connections).

Supplementary Table 4

GC-MS product analysis of the PET pyrolysis reaction by STH using a 0.11 s heating duration at ~26 V in a period of 1.10 s.

Retention Time (min)	Chemical Name	Area (%)
7.005	Styrene	0.91
8.793	2-Hydroxy-acetic acid	3.46
10.570	4-Hydroxy-4-methyl- 2-pentanone	0.39
10.643	Indene	0.42
11.327	Oxanilic acid	0.85
11.864	Octyl alcohol	6.55
13.335	Azulene	1.55
14.313	Benzoic acid	19.57
14.829	Glycerol	0.94
16.152	2-Methyl- benzoic acid	2.07
17.754	4-Ethylbenzoic acid, methyl ester	0.63
18.099	3-Phenyl- 2-propenoic acid	1.47
20.757	1,2,3-Benzenetricarboxylic acid, trimethyl ester	4.32
21.241	1,4-Benzenedicarboxylic acid, monomethyl ester	0.80
21.835	1,4-Benzenedicarboxylic acid, 1-ethenyl ester	6.16
24.122	1,4-Benzenedicarboxylic acid	42.99
26.284	1,2-Benzenedicarboxylic acid, monoethyl ester	6.17
28.001	Fenbufen	0.75

Supplementary Discussion 1

Thermogravimetric analysis was conducted using a Discovery SDT 650 instrument from room temperature to 1000 °C with a ramping rate of 5 °C/min. PP displays apparent weight loss at ~420 °C (Supplementary Figure 1), suggesting that volatile species start to form at this temperature.

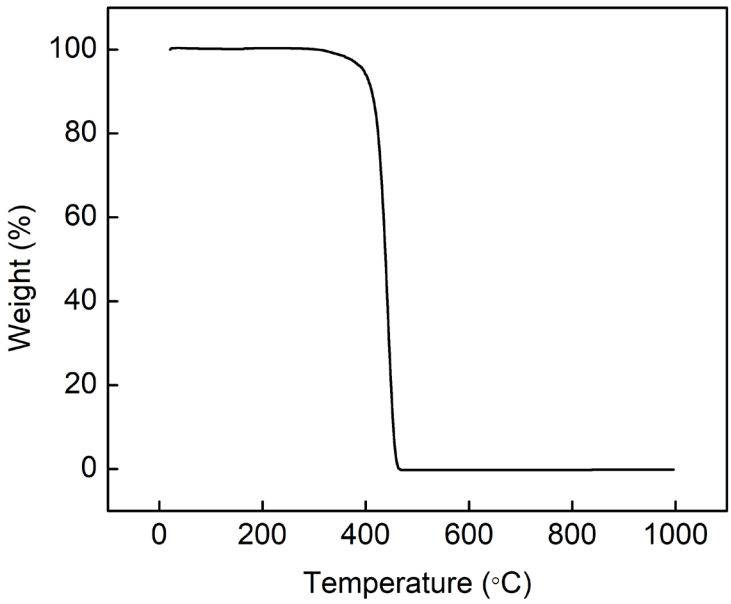

Supplementary Figure 1. Thermal gravimetric analysis of the PP starting material.

Supplementary Discussion 2

The role played by the bilayer structure is critical for STH as it creates a temperature gradient that ensures a continuous melting, wicking, vaporization, and reaction process (Supplementary Figure 2a). If instead of a heater/reactor bilayer design we were to use a single carbon layer to heat the entire plastic melt in the container (Supplementary Figure 2b), there would be no temperature gradient to promote the wicking effect. In this case, the single heater layer would primarily heat the reactant directly within the reservoir, where the thermal inertia of the large volume of the reactant would prevent the temperature profile of the material (e.g., heating and cooling rate, timescale) from closely following that of the heater, resulting in poor control of the reaction progress. In comparison, the temperature gradient produced by the heater/reactor bilayer structure promotes the plastic wicking mechanism, which gradually and continuously supplies small amounts of reactant into the pores of the reaction zone. As the wicked reactant in these pores has lower mass and therefore lower heat capacity, the temperature profile of the wicked reactant can better synchronize with that of the heater, which can allow us to more accurately control the reaction pathway of the reactant. Additionally, the gradual wicking and diffusion of the reactants through the porous reactor layer allow the intermediate products to have longer residence times and thereby experiencing more heating pulses compared to the operation using single heater layer, which should increase the degree of depolymerization and the monomer yield.

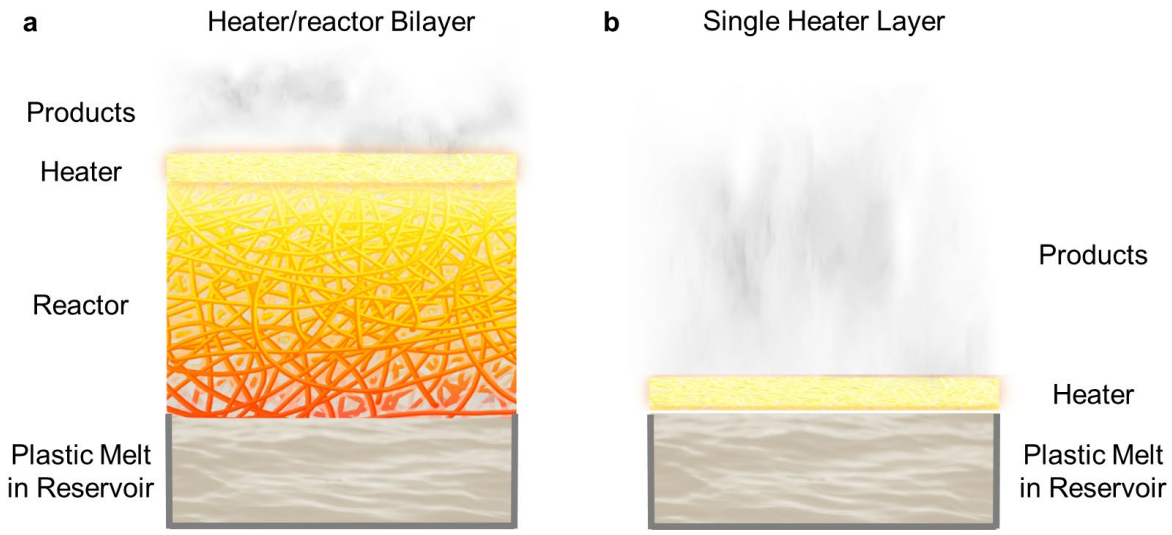

Supplementary Figure 2. Schematic comparing (a) the reaction setup using the heater/reactor bilayer structure and (b) the setup using a single heater layer structure (i.e., without the reactor layer).